23th IAEA Fusion Energy Conference,
Daejeon, Korea, 11-16 Oct., 2010
PD/P-01

Role of Low-Order Rational Surfaces in Transport Barrier Formation on the Large Helical Device

K. Toi, F. Watanabe[a], K. Tanaka, T. Tokuzawa, K. Ogawa[b], M. Isobe, M. Osakabe, Y. Suzuki, T. Akiyama, K. Ida, M. Goto, K. Kawahata, T. Morisaki, S. Morita, K. Narihara, S. Ohdachi, S. Sakakibara, H. Urano[c], I. Yamada, M. Yoshinuma and LHD Experiment Group

National Institute for Fusion Science, 322-6 Oroshi-cho, Toki, Japan
[a] Faculty of Energy Science, Kyoto University, Kyoto, Japan
[b] Faculty of Engineering, Nagoya University, Nagoya, Japan
[c] Japan Atomic Energy Agency, Naka, Japan

E-mail: toi@lhd.nifs.ac.jp

Abstract

In the Large Helical Device, edge transport barrier (ETB) was formed by H-mode transition near the low-order rational surfaces, that is, at the $\iota/2\pi=1$ resonant layer ($\iota/2\pi$: the rotational transform) in outward-shifted plasmas of R_{ax}=3.9m (R_{ax}: the magnetic axis position in the vacuum field), and the $\iota/2\pi=2$ resonant layer in inward-shifted plasmas of R_{ax}=3.6m. The $\iota/2\pi=1$ and 2 resonant layers reside in the stochastic field region existing just outside the last closed magnetic surface (LCFS). In the outward-shifted plasmas, H-modes without edge localized modes (ELM-free H-modes) followed by giant ELMs were obtained, while H-modes with high frequency and low amplitude ELMs were obtained in the inward-shifted plasmas. A new type of barrier formation induced by TAE bursts was observed in the plasmas of R_{ax}=3.6m, where the transport barrier is formed near the $\iota/2\pi=1$ surface locates inside LCFS.

1. Introduction

Confinement improvement in stellarator/helical plasmas as well as tokamak plasmas is realized by formation of transport barrier in the plasma edge and/or core regions. Edge transport barrier (ETB) and internal transport barrier (ITB) are formed when plasma heating power exceeds a certain threshold. ETB in tokamaks develops just inside the last closed flux surface (LCFS), suddenly steepening the gradient of plasma pressure there [1]. On the other hand, ITB is formed near the zero shear layer in a reversed-shear tokamak plasma [2] or at low-order rational surfaces such as the safety factor q=2 or 3 [3]. Effect of low-order rational surface on ITB formation is not clearly understood. Moreover, the effect on ETB formation is not much investigated in tokamaks, because the rotational transform $\iota/2\pi$ (=1/q) rapidly decreases down to low value in the plasma edge having high magnetic shear, in particular poloidal divertor tokamak. This effect was investigated in TJ-II stellarator [4]. However, the rational surface effects will not be localized near the edge due to low magnetic shear. The effects of low-order rational surfaces on transport barrier formation should be clarified

for better understanding of anomalous transport and transport barrier formation mechanisms.

The Large Helical Device (LHD) has an advantage for studying the effects of low-order rational surfaces on ETB formation. In contrast to tokamak plasmas, the rotational transform rapidly increases to close or more than unity in the plasma edge. Accordingly, low-order rational surfaces such as $\iota/2\pi$=1 and 2 reside in the edge region where ETB grows. Moreover, the locations of $\iota/2\pi$=1 and $\iota/2\pi$=2 are easily shifted from the plasma core region to outside LCFS or vice versa by changing the magnetic axis position in the vacuum field R_{ax}. When R_{ax} is scanned from 3.6m to 3.9m, the location of the $\iota/2\pi$=1 surface moves from well-inside LCFS to stochastic field region (SR) which is just outside the LCFS. The $\iota/2\pi$=2 layer always stays in the SR. It is predicted from the calculations by a 3D MHD equilibrium code HINT2 that the SR of LHD plasmas in the vacuum field persists without healing and tends to expand with increase in the beta value [5]. That is, the SR evaluated in the vacuum is thought to be the minimum size in LHD plasmas. Moreover, effects of SR on ETB formation can be investigated because of a unique character of LHD magnetic configuration.

This paper presents experimental results on ETB characteristics observed in R_{ax}-scan experiments in LHD. In addition, transport barrier formation induced by TAE bursts is also presented. The effects of low-order rational surfaces on the TAE-burst triggered barrier are also discussed.

2. Characteristics of L-H Transition and ELMs

In the R_{ax}-scan experiments, it has been found that L-H transition, ETB location and ELM behaviors are sensitively dependent on R_{ax}. In an outward-shifted configuration of R_{ax}=3.9m at the toroidal field B_t=-0.9T, ELM-free H-modes were obtained, as shown in Fig.1(a). The negative sign of Bt means the counter clockwise direction of the toroidal filed. The ELM free phase with linear increases in the line-averaged electron density $\langle n_e \rangle$ and the plasma stored energy W_p was terminated by giant ELMs which are excited in the late H-phase. Note that absorbed NBI power is stepped down at t=5.0s in the ELM free phase. Line-integrated electron densities increase at various vertical chords inside the edge transport barrier formed at the L-H transition of which signals are marked as "$n_eL(r/a\sim0)$" and "$n_eL(r/a=0.5)$" , and decrease at those outside ETB, marked as "$n_eL(r/a)>1$"(Fig.1(b)). Magnetic fluctuations including coherent and incoherent components less than 50 kHz were clearly suppressed, as shown in Fig.1(c). Figure 2 shows radial profiles of electron temperature and density just before (t=4.8s) and after (t=4.9s) the transition (t=4.87s), where these profiles are measured in horizontally elongated section with a multichannel Thomson scattering system [6]. This figure also shows the density increment across the transition, that is $\Delta n_e = n_e(t=4.9s) - n_e(t=4.8s)$. The ETB foot defined by the radial profile of Δn_e locates near the $\iota/2\pi$=1 layer that locates in stochastic field region outside LCFS (Fig.2). In the H-phase after the transition, Δn_e increases in the edge region and also in the core region. Electron density fluctuations measured with CO_2 laser phase contrast imaging (PCI) [7] and millimeter wave reflectometer [8] are also clearly suppressed across the transition.

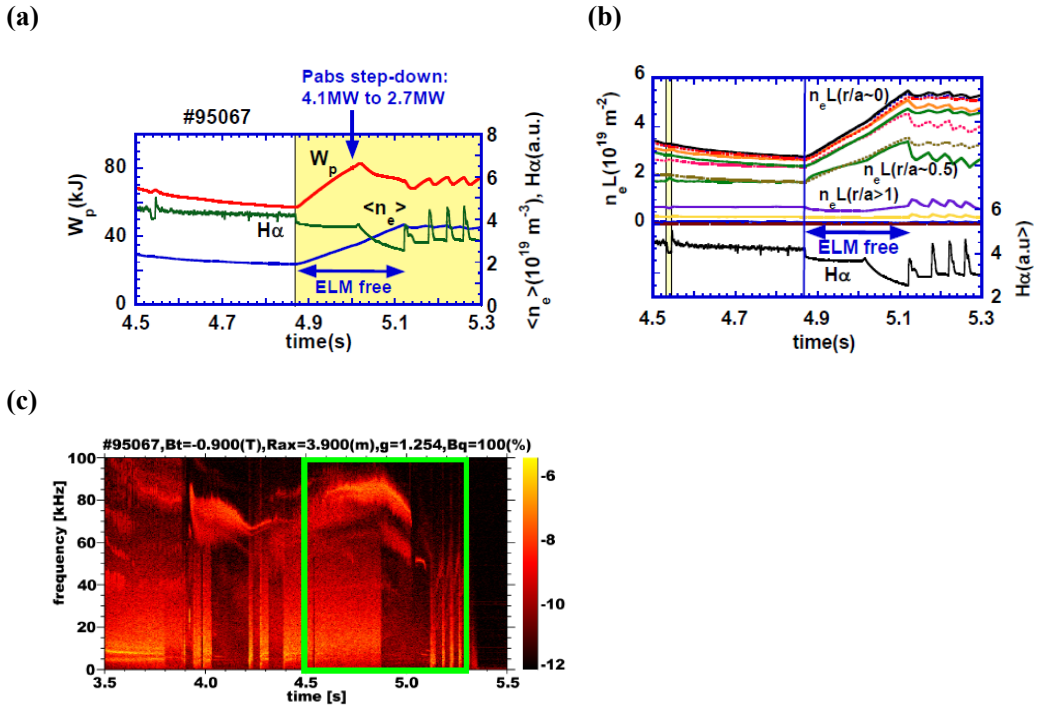

Fig.1(a) Time evolution of the plasma stored energy W_p, line-avearged electron density $<n_e>$ and H_α emission in an ELM free H-mode obtained in an outward-shifted plasma of R_{ax}=3.9m, where the toroidal field strength at the magnetic axis B_t=-0.9T (negative means in counter clock-wise direction). (b) Time evolution of line-integrated electron densities at various lines of sight in the vertically elongated section. (c) Spectrogram of magnetic probe signal, where the rectangular green frame indicates the time windows in Figs.1(a) and (b).

The phase velocity of the density fluctuations was also measured with the PCI system. In Fig.3, the contour plots of the density fluctuation amplitude are shown for three typical time windows of 10ms: (a) in L-phase, (b) after the L-H transition and (c) in deep H-phase, in the plane of the normalized minor radius ρ and the poloidal phase velocity v. In the L-phase, strong density fluctuations near the edge (ρ~1) with ~-2.5km/s are clearly suppressed, and the phase velocity is increased to ~-6.5km/s, where the negative phase velocity stands for the velocity in electron

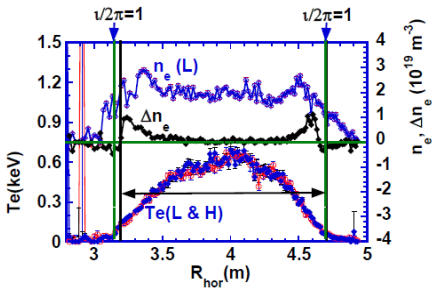

Fig.2 *Radial profiles of electron temperature T_e and density n_e along the major radius in the horizontally elongated section, in the L-phase. The increment of electron density just after the transition Δn_e is also shown. The T_e-profile remains unchanged across the transition. The vertical solid lines indicate the LCFS in the vacuum field. The vertical arrows indicate the location of the $\iota/2\pi$=1 resonant layer in the stochastic layer. The horizontal arrow indicates the nested magnetic surface area in the vacuum field.*

diamagnetic drift direction. After about 130~140ms later from the transition, the phase velocity is further increased to ~-8.5km/s. These phase velocity in the laboratory frame is increased across the transition. This is thought to indicate enhanced *ExB* drift, that is, the radial electric field is Er~-2 kV/m, where negative E_r means the radial electric field pointing to the interior. After the transition, E_r increases to ~-5.5 kV/m and further increases ~-7 kV/m in H-phase after ~130ms later from the transition. In the L-phase, the radial electric field in the edge where ETB will be formed is negative but considerably small. After the transition, E_r is enhanced but still weak. The shear of E_r is also considerably small in the H-phase. This fact may be a reason why the ETB is formed in stochastic field region.

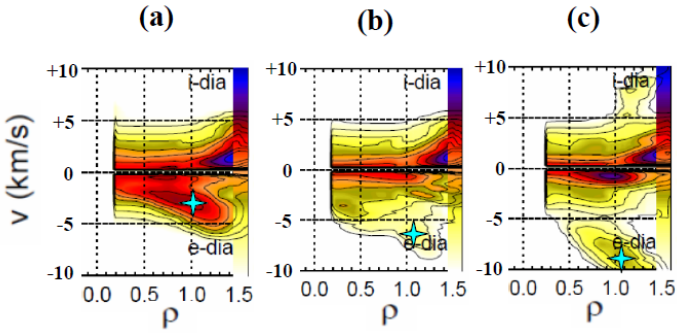

Fig.3 Amplitude and phase velocity v of electron density fluctuations measured by CO_2 laser phase contrast imaging technique as a function of the normalized minor radius, at the L phase (a) and H-phases (b) and (c). The time windows at the three cases are respectively set as (a)Δt_{LH}=-30ms ~ -20ms, (b) +20ms~+30ms and (c) +130ms ~ +140ms. The characteristic fluctuation peak propagates in the electron diamagnetic drift direction is marked with a blue cross.

On the other hand, the H-modes having high frequency and small amplitude ELMs were obtained in inward-shifted configurations of R_{ax}=3.6m, as shown in Fig.4(a). Just after the transition the plasma stored energy and line averaged electron density suddenly jump up, exhibiting a sudden depression of Hα emission and high frequency small-amplitude modulations (ELMs). In contrast to the above-mentioned ELM free plasma, coherent and incoherent magnetic fluctuations less than 50 kHz are enhanced noticeably. Enhanced coherent magnetic fluctuations have m/n=2/3 and 1/2 mode structures. They are thought to be resistive interchange modes destabilized in the edge, because the ETB region is in the magnetic hill. Density fluctuations measured by the PCI system are strongly enhanced just after the transition. Note that fluctuations propagate in the ion diamagnetic drift direction are suppressed by a factor of two, while those propagate in the electron diamagnetic drift direction are considerably enhanced similar to the behavior of magnetic fluctuations. As seen from Fig.4(b), the ETB foot derived from Δn_e locates near the $\iota/2\pi$=2 resonant layer. Note that the resonant layer resides obviously in the stochastic field region defined by the vacuum field. We also calculated the MHD equilibrium without assuming the existence of nested magnetic surfaces by a 3D plasma MHD equilibrium calculation code HINT2 [9]. The HINT2 code demonstrated that the stochastic field layer exists in the vacuum field persists and even expand radially. In conclusion, ETB locations in both inward and

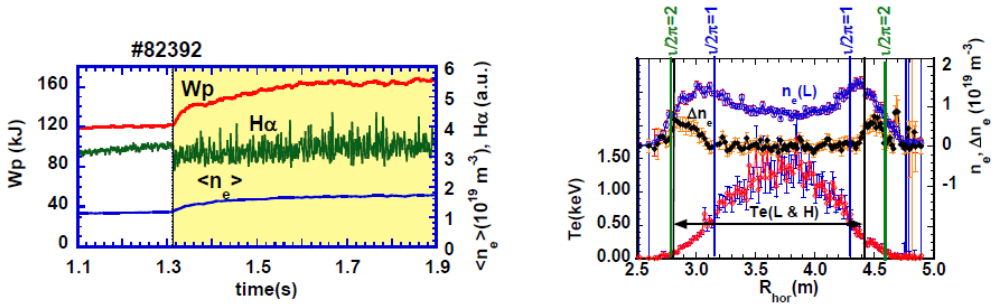

Fig.4 (a) Time evolution of the plasma stored energy W_p, line-averaged electron density $<n_e>$ and H_α emission in an H-mode with high frequency small ELMs obtained in the inward-shifted plasma of Rax=3.6m, where the toroidal field strength at the magnetic axis Bt=-0.9T (negative means the counter clock-wise direction). (b)Radial profiles of electron temperature T_e and density n_e along the major radius in the horizontally elongated section, in the L-phase of an H-mode plasma obtained in the inward-shifted configuration of Rax=3.6m. The increment of electron density just after the transition Δn_e is also shown. The T_e-profile remains unchanged across the transition. The vertical solid lines indicate the LCFS in the vacuum field. The dotted vertical lines indicate the location of the the $\iota/2\pi=1$ and 2 resonant layers in the stochastic layer, respectively.

outward-shifted configurations are in stochastic field region in ETB plasmas with finite beta. Usually, the plasma potential profile over the stochastic field region will not have any gradient, that is, almost no E_r or fairly small E_r is inferred. Actually, the poloidal velocity of a plasma measured by charge exchange recombination spectroscopy [10] was very small (~+1 km/s), which is equivalent to ~0.8kV/m just before the L-H transition (Fig.5). The poloidal velocity is enhanced modestly to ~-3km/s 35 ms after the transition, which corresponds to ~-2.6kV/m. These small changes in poloidal rotaion at the ETB region are thought to be due to the formation of ETB in the stochastic field region.

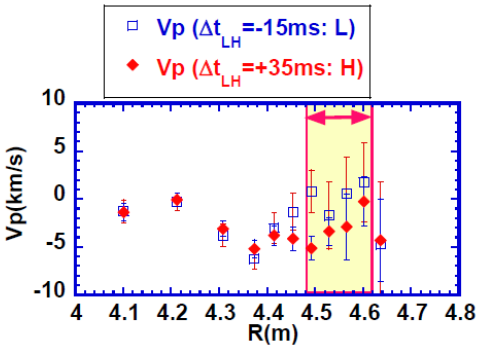

Fig.5 Radial profiles of poloidal rotation velocity measured by charge exchange spectroscopy in L and H phases of a similar H-mode plasma with that shown in Fig.4(a). The shaded zone indicates the ETB region determined from Fig.4(b).

Edge regions of both magnetic configurations are in the magnetic hill at any toroidal beta values, and resistive interchange modes (RICs) are easily destabilized when the pressure gradient exceeds a certain critical gradient. Therefore, the critical pressure gradient would depend upon a destabilizing factor: magnetic hill height and several stabilizing factors such as the magnetic shear and diamagnetic drift [11, 12]. Thus excited RICs effectively reduce the pressure gradient generating a magnetic-island like

flatted region through nonlinear evolution [12]. Nonlinear saturation of RICs will be determined by competition between effective reduction of the pressure gradient and the other stabilizing factors mentioned above, sometimes exhibiting the amplitude modulation. In this process, the pressure gradient is steepened at the both sides in the O-point. The poloidallly localized pressure gradient may generate the radial electric field at the resonant layer [13], or generate convective cell [14]. These processes may trigger the L-H transition and lead to ETB formation. We discuss the reason why ELM free phase is sustained for much longer time in the configuration of R_{ax}=3.9m than that in the R_{ax}=3.6m configuration. The relative magnitude of the pressure gradient achieved at ETB in the R_{ax}=3.9m configuration plasma (Fig.1(a)) is by about 30 % larger than that in the R_{ax}=3.6m configuration (Fig.4(a)). The rise rate of the edge pressure gradient just after the L-H transition can be approximately evaluated by that of the plasma stored energy |dWp/dt|, where Wp is the stored energy. In the Rax=3.9m and 3.6m configurations, the relative rise rate $|dWp/dt|/P_{dep}$ is ~0.05 and 0.2, respectively. The differences in the critical pressure gradient and the rise rate of the pressure gradient suggest that the duration of ELM free phase in the Rax=3.9m configuration would be ~5 times longer than that in the Rax=3.6m configuration. The ELM free phase in the former configuration is predicted to last ~100 ms with the fixed NBI absorbed power for that in the latter one, ~10 ms. The longer duration of ELM free phase in the former configuration is still about two times longer than that in the former. In the former configuration, additional other stabilization effects may contribute to enhanced stability of the ETB region.

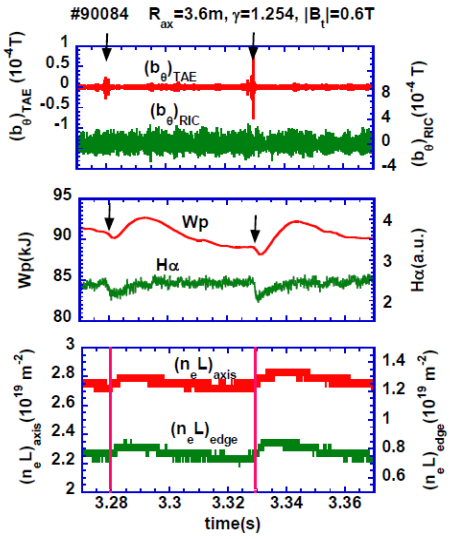

Fig.6 Time evolutions of magnetic fluctuations of TAE and RIC, W_p, H_α, and line-integrated electron densities at the magnetic axis and the edge, in a high beta plasma where a transient confinement improvement is triggered by TAE bursts.

3. Confinement Improvement by TAE Burst

Recently, effects of TAEs on bulk plasma confinement attract much attention. In NBI heated high beta plasmas of R_{ax}=3.6m at lower B_t=-0.6T, n=1 TAE bursts often induce transient improvement of global energy confinement, as shown in Fig.6. The stored energy W_p rises obviously by each TAE burst, having a sharp drop in Hα-emission. The line integrated electron density and soft X-ray emission (SX) also rise up by each TAE burst, similar to W_p. The transport barrier location evaluated by the change of the SX emission profile is near the $\iota/2\pi$=1 surface, as shown in Fig.7. The formed transport barrier was sustained for a time scale, comparable to the global energy confinement

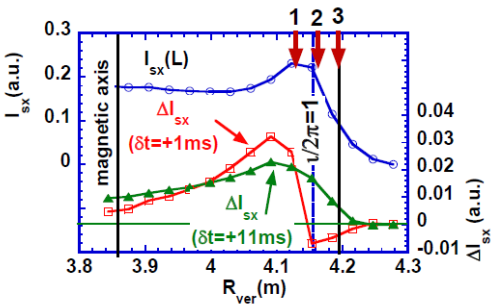

Fig.7 Soft X-ray emission and the increment of the emission by a TAE burst as a function of major radius in a vertically elongated section.

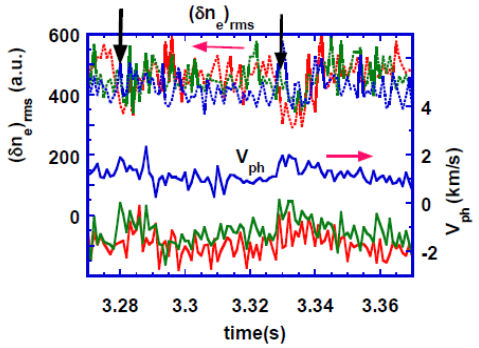

Fig.8 Time evolutions of density fluctuation amplitude and the phase velocity measured with CO_2 laser phase contrast imaging. By every TAE burst shown by vertical arrows, the phase velocity is enhanced in the ion diamagnetic drift direction.

time (~10-20 ms). Just after a TAE burst, density fluctuations in drift-wave ranges, which are measured by CO_2 laser phase contrast imaging (PCI) [7], decrease by about 20-30% at r/a~0.8 (the arrow 1 in Fig.7) near the ι/2π=1 surface, as shown in Fig.8. The phase velocity increases more clearly at r/a~0.9 (the arrow 2 in Fig.7), in the ion diamagnetic direction. The TAE eigenfunction peak is in r/a~0.6-0.7. The enhanced phase velocity and the direction can be explained by momentum input by TAE-induced loss/redistribution of energetic ions. Shear flow generation by non-ambipolar radial transport of energetic ions may play a role in this process [15]. So far, this transient improvement of bulk plasma confinement is not observed in the plasmas of R_{ax}=3.9m. The ι/2π=1 surface in the nested magnetic surface region may be favorable for triggering an internal transport barrier formation by TAE bursts.

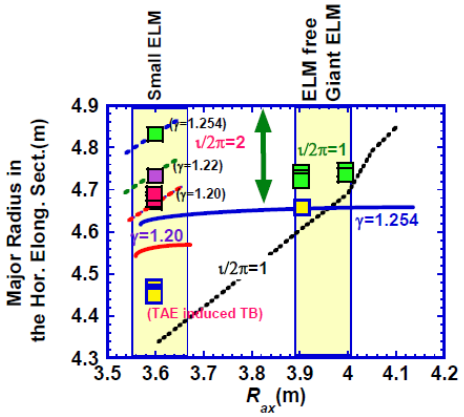

Fig.9 Dependence of the ETB location in the outboard side on the the magnetic axis position R_{ax}. Blue and red solid curves stand for the LCFS at γ=1.254 and 1.2, respectively. A dotted curve indicates the location of ι/2π=1 surface in the vacuum field. Broken blue, green and red curves indicate the ι/2π=2 layer at γ=1.254, 1.22 and 1.2, respectively. Squares show the observed positions of ETB foot in various configurations of R_{ax}, and clearly are in stochastic field region outside LCFS. The location of the transport barrier formed by TAE bursts is also shown.

4. Conclusion

In LHD, characteristics of ETB formation and ELMs sensitively depend on

the magnetic axis position in the vacuum field R_{ax} of which value can easily adjust the low order rational surfaces such as $\iota/2\pi=1$ at the plasma formation. Although H-modes in the inward-shifted configuration R_{ax}=3.6m always have high frequency and low amplitude ELMs, H-modes in the outward-shifted configuration R_{ax}=3.9m have an ELM free phase much longer than global energy confinement time, of which phase is terminated by singular giant ELMs. The most significant finding is that ETB is formed by H-mode transition near the low-order resonant layers in the stochastic magnetic field region, that is, at the $\iota/2\pi=1$ resonant layer in the outward-shifted plasmas of R_{ax}=3.9m, and the $\iota/2\pi=2$ resonant layer in the inward-shifted ones of R_{ax}=3.6m. A new type of barrier formation by TAE bursts was observed in the plasmas of R_{ax}=3.6m, where the transport barrier is formed near the $\iota/2\pi=1$ surface located in the nested magnetic surface region inside LCFS. However, so far this type of transition by TAE bursts is not observed in the configuration of R_{ax}=3.9m, where the $\iota/2\pi=1$ surface is in the stochastic field region. These results suggest that the resonant surfaces/layers such as $\iota/2\pi=1$ and 2 play an important role in transport barrier formation in LHD. The locations of ETB formed with L-H transition and the transport barrier by TAE bursts are summarized in Fig.9.

Acknowledgements

The authors acknowledge the LHD experimental team for their excellent supports to this research. This work is supported in part by the Grant-in-Aid for Scientific Research from MEXT: No. 16082209 and from JSPS: No. 16656287, No. 15206107 and No. 21360457, and the LHD project budget (NIFS10ULHH011). This research is also supported by the JSPS-CAS Core-University Program in the field of “Plasma and Nuclear Fusion”.

References

[1] E.J. Doyle et al., Nucl. Fusion **47,** S18(2007).
[2] J. Conner et al., Nucl. Fusion **44**, R1 (2004).
[3] Koide, Y. et a., Phys. Rev. Lett. **72,** 3662 (1994).
[4] Estrada, T et al., Contrib. Plasma Phys. **50**, 501 (2010).
[5] Y. Suzuki et al., Plasma Fus. Res. **4**, 036 (2009).
[6] K. Narihara et al., Rev. Sci. Instrum., **74**, Part II, 3878 (2004).
[7] K. Tanaka et al., Rev. Sci. Instrum., **79**, 10E702 (2008).
[8] T. Tokuzawa et al., Fusion Sci. Technol. **58**, 364 (2010).
[9] Y. Suzuki et al.,Nucl. Fusion **46**, L19 (2006).
[10] M. Yoshinuma et al., Fusion Sci. Technol. **58**, 375 (2010).
[11] Diamond et al., Phys. Rev. Lett. 72, 2565 (1994).
[12] K. Ichiguchi et al., Nucl. Fusion **43, 1101** (2003).
[13] L. Garcia et al., “*On the Role of Rational Surfaces on Transport in Fusion Plasmas*”, Proc. 18th IAEA Fusion Energy Conference, Sorrento, Italy, 4 to 10 Oct. 2000, paper No. IAEA-CN-77/EXP5/07.
[14] C.J. McDevitt and P.H. Diamond, Phys. Plasmas **14**, 112306 (2007).
[15] K.L. Wong et al., Nucl. Fusion **45**, 30 (2005).